Disruption of Broca's Area Alters Higher-order Chunking Processing during Perceptual Sequence Learning

Andrea Alamia[1*], Oleg Solopchuk[1*], Alessandro D'Ausilio[2], Violette Van Bever[1], Luciano Fadiga[2,3], Etienne Olivier[1,2], and Alexandre Zénon[1]

Abstract

■ Because Broca's area is known to be involved in many cognitive functions, including language, music, and action processing, several attempts have been made to propose a unifying theory of its role that emphasizes a possible contribution to syntactic processing. Recently, we have postulated that Broca's area might be involved in higher-order chunk processing during implicit learning of a motor sequence. Chunking is an information-processing mechanism that consists of grouping consecutive items in a sequence and is likely to be involved in all of the aforementioned cognitive processes. Demonstrating a contribution of Broca's area to chunking during the learning of a nonmotor sequence that does not involve language could shed new light on its function. To address this issue, we used offline MRI-guided TMS in healthy volunteers to disrupt the activity of either the posterior part of Broca's area (left Brodmann's area [BA] 44) or a control site just before participants learned a perceptual sequence structured in distinct hierarchical levels. We found that disruption of the left BA 44 increased the processing time of stimuli representing the boundaries of higher-order chunks and modified the chunking strategy. The current results highlight the possible role of the left BA 44 in building up effector-independent representations of higher-order events in structured sequences. This might clarify the contribution of Broca's area in processing hierarchical structures, a key mechanism in many cognitive functions, such as language and composite actions. ■

INTRODUCTION

Mastering the myriad of behaviors that make humans distinctive, such as language, tool use, and music, relies on the ability to learn, encode, and process perceptual, cognitive, or motor sequences (Perruchet & Pacton, 2006; Corballis, 2003; Janata & Grafton, 2003; Keele, Ivry, Mayr, Hazeltine, & Heuer, 2003; Conway & Christiansen, 2001). Regardless of their nature, whether these sequences are arbitrary, hierarchically organized, or characterized by some regularities leading to statistical learning (Keele et al., 2003; Conway & Christiansen, 2001), a common mechanism known as "chunking" seems to underlie sequence learning (Gobet et al., 2001). A chunk can be defined as a unit in a "maximally compressed code" (Mathy & Feldman, 2012), and chunking is regarded as a way to facilitate learning and to optimize performance by lowering memory load (Penhune & Steele, 2012; Huntley, Bor, Hampshire, Owen, & Howard, 2011; Bor, Duncan, Wiseman, & Owen, 2003; Sakai, Kitaguchi, & Hikosaka, 2003; Rosenbaum, Kenny, & Derr, 1983). More recently, it has even been suggested that because chunking permits the detection and encoding of regularities between items in working memory, it might also play a role in consciousness (Bor & Seth, 2012). From a behavioral point of view, chunking is characterized by a typical pattern of RTs to the different sequence items, depending on their position in a chunk. Indeed, retrieving a chunk comes at the cost of longer RTs when processing the first item, possibly because it is accompanied by the retrieval of the subsequent chunk elements (Clerget, Poncin, Fadiga, & Olivier, 2012; Pammi et al., 2012; Verwey & Abrahamse, 2012; Sakai et al., 2003; Verwey & Eikelboom, 2003; Koch & Hoffmann, 2000). Supposedly, chunking makes the processing and learning of sequences more efficient (Verwey, 2010; Bor et al., 2003; Sakai et al., 2003; Koch & Hoffmann, 2000), although chunking is not always a good predictor of performance or learning (Clerget et al., 2012; Wymbs, Bassett, Mucha, Porter, & Grafton, 2012).

The neural correlates of chunking remain poorly understood. Numerous brain regions have been found to be activated during sequence learning (Penhune & Steele, 2012; Doyon et al., 2009; Ashe, Lungu, Basford, & Lu, 2006; Keele et al., 2003; Hikosaka, Nakamura, Sakai, & Nakahara, 2002), but studies that thoughtfully examined the neural correlates of chunking are rare. Among the brain regions activated during sequence learning is the ventrolateral pFC (VLPFC), including Broca's area, which is known to be involved in diverse tasks requiring sequence processing, including hierarchical processing

[1]Université catholique de Louvain, [2]Fondazione Istituto Italiano di Tecnologia, Genova, Italy, [3]University of Ferrara
*These two authors contributed equally to this work.

Journal of Cognitive Neuroscience 28:3, pp. 402–417
doi:10.1162/jocn_a_00911

(Clerget, Andres, & Olivier, 2013; Bahlmann, Schubotz, Mueller, Koester, & Friederici, 2009; Koechlin & Jubault, 2006; Schubotz & Fiebach, 2006; Grossman, 1980), sequence representation (Clerget, Badets, Duqué, & Olivier, 2011; Dominey, Hoen, Blanc, & Lelekov-Boissard, 2003), and action sequencing (Clerget, Winderickx, Fadiga, & Olivier, 2009; Fazio et al., 2009). In addition, a few neuroimaging studies suggest that Broca's area is also involved in chunk processing (Pammi et al., 2012; Wymbs et al., 2012). In a recent TMS study, we postulated that the posterior part of Broca's area (the left Brodmann's area [BA] 44) might integrate higher-order chunks (Clerget et al., 2012) while learning a motor sequence in a serial RT task.

The goal of this study was to test this prediction by seeking experimental evidence for the contribution of the left BA 44 in encoding higher-order relations between chunks in a nonmotor and nonlinguistic sequence. To do so, we took advantage of continuous theta burst stimulation (cTBS; Huang, Edwards, Rounis, Bhatia, & Rothwell, 2005) applied over the left BA 44 to disrupt the neural activity of this area in healthy participants before they learn a perceptual sequence. The systematic relation between consecutive items of the sequence was carefully controlled, so that it yielded a strongly structured sequence with different, clearly identifiable hierarchical levels (Koch & Hoffmann, 2000) that could be reliably chunked by most, if not all, participants. As a control, we performed the same experiment in a separate group of participants with cTBS applied over the vertex. Using a between-subject design was mandatory because the chunking pattern evolves during the course of sequence learning (Clerget et al., 2012; Wymbs et al., 2012), making it impossible to test the same participants twice in the same task.

METHODS

Participants

Altogether, we recruited 30 neurologically normal participants, and the final data set (see below) included 24 participants (mean age = 23 ± 4 years, 12 women), 12 in each group. All participants were right-handed, as assessed by the Edinburgh Handedness Inventory (Oldfield, 1971), and had normal or corrected-to-normal vision. Written informed consent was obtained from each participant. The experiment was conducted according to the Declaration of Helsinki and approved by the ethics committee of the Université catholique de Louvain. The participants received financial compensation to participate in this study.

Experimental Setup and Design

The experiment took place in a quiet and dimly lit room. The volunteers sat in an armchair in front of a personal computer. Before participating in this study, each participant was seen by a neurologist to minimize the potential risk of their experiencing an adverse reaction to TMS (Keel, Smith, & Wassermann, 2001). The experiment was controlled by a Matlab program (The MathWorks, Inc., Natick, MA). To avoid imprecision in measurement of RT because of the delays inherent in Microsoft Windows, we used a homemade device allowing us to detect keypresses with submillisecond accuracy. Briefly, this device contains a microcontroller (MSP430F249, Texas Instruments, Inc., Dallas, TX), which combines both Video Graphics Array and keyboard inputs; in this particular case, the display of the imperative stimulus triggered an internal clock, which was stopped by a keyboard event (keypress). The microcontroller then sent both the key code and the clock value (128 μsec temporal resolution) to the computer via a USB interface.

The experiment comprised four stages: (1) a control task block (CT1), (2) cTBS application, (3) the main task (eight blocks), and (4) a second control task block (CT2). Following the cTBS application, the participant remained seated for around 5 min before moving to the experimental setup in the same room.

Main Task

The design of the sequence used in this experiment builds on a study by Kühn (2011). Participants had to learn, explicitly, by trial and error, a 16-element sequence characterized by a systematic relational structure among the items that constituted it (Koch & Hoffmann, 2000; Figure 1A). The sequence was designed in such a way that it should be chunked comparably by all participants: Indeed, the main sequence could be parsed into two subsequences of eight digits, each with the same relational structure (32322323-41411414). These subsequences could again be parsed into two quadruplets related to each other by inversion (3232-2323 and 4141-1414), and each quadruplet could be further divided into two identical pairs (32-32, 23-23 and 41-41, 14-14). Therefore, this sequence allowed us to distinguish among four relational levels between the stimuli, referred to as "chunking levels" hereafter. The different chunking levels are illustrated in Figure 1A, in red (Level 1), yellow (Level 2), green (Level 3), and gray (Level 4). The statistical analysis performed on all items belonging to the same hierarchical levels showed a strong influence of hierarchical level on RT [see Figure 1B, main effect of Level, $F(3, 66) = 13.91$, $p < .0001$; see Results for detail], clearly demonstrating the effectiveness of the sequence structure manipulation on RT.

The sequence was repeated five times in each block, and the participants performed eight blocks, leading to 40 sequence repetitions across the whole experiment. Importantly, participants were not informed about the sequence structure. Each sequence started with the display of a central fixation cross for 2000 msec, followed by

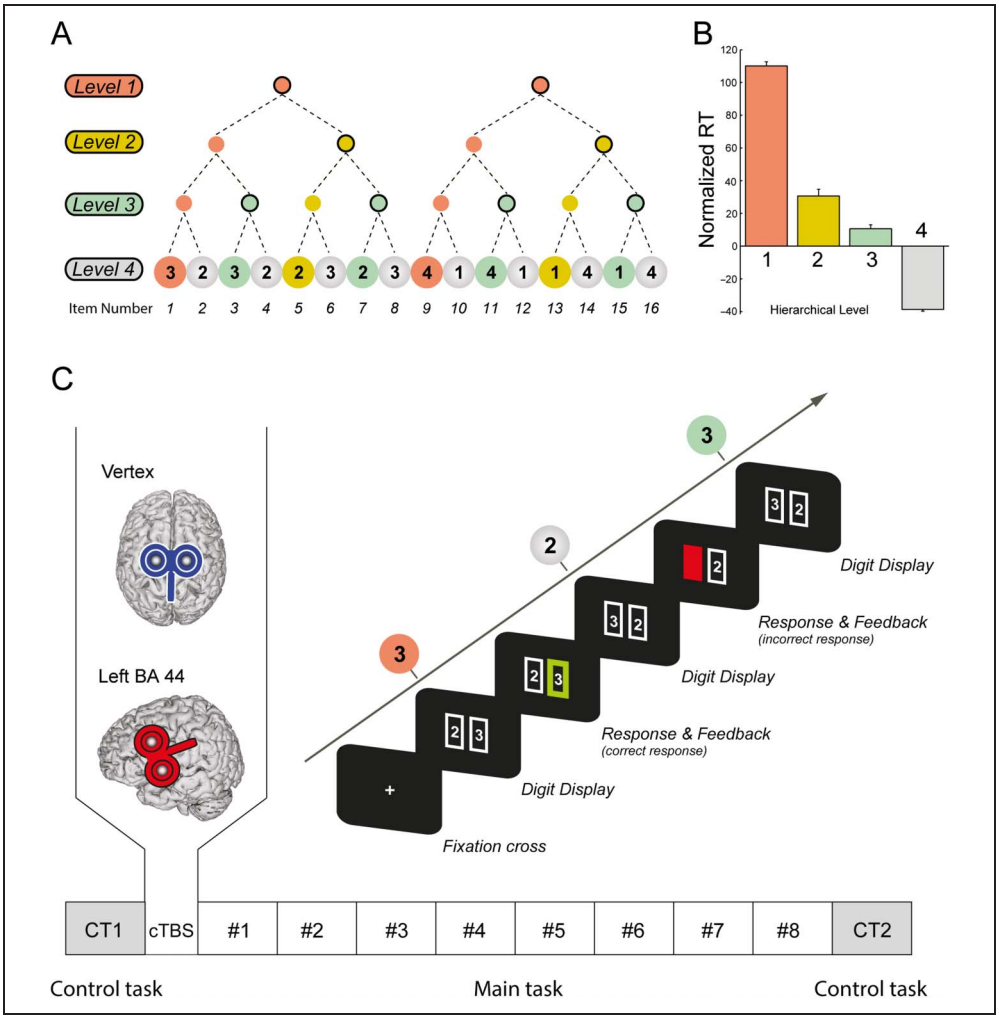

Figure 1. Sequence and experimental procedure. (A) The sequence to be learned contained 16 elements and was characterized by a particular relational structure, so it could be chunked consistently by all participants according to four distinct levels, indicated in red (Level 1), yellow (Level 2), green (Level 3), and gray (Level 4). (B) Average RT within each hierarchical level (normalized with respect to the mean RT of each block to account for the learning effect). Same color convention as in A. (C) Time course of a sequence and design of the experiment. Each sequence started with the display of a fixation cross for 3000 msec, followed by the display of a first pair of stimuli (digits in a rectangle). The participant had to select the digit belonging to the sequence by pressing the appropriate response key (right index or right middle finger). This was followed by feedback consisting of a green rectangle surrounding the selected digit for a correct response or a red mask for an incorrect one. Then the next pair of digits was displayed. After the completion of one sequence (i.e., 16 consecutives trials), a fixation cross appeared again for 2000 msec, indicating the onset of the next sequence. Each block comprised five sequence repetitions. The lower part of the figure illustrates the experimental design. The experiment started with the first control task (CT1), which had the same design as the main task except that the four digits were replaced by for four letters (A, B, C, and D) and there was no sequence to learn ("B" was always the correct response). It was followed by the application of cTBS either over either the left BA 44 or the vertex (control group). Then, the participants performed the main task (8 blocks × 5 sequences), and the control task was repeated (CT2) at the end of the experiment.

the simultaneous presentation of two rectangles (white border contrasted against a black background, 9.5° width and 13.4° height) arranged horizontally on either side of the screen center (Figure 1C). Two digits (from 1 to 4) were displayed on the screen, one in each rectangle: One digit belonged to the sequence to be learned ("target" digit), whereas the other was selected at random. Importantly, the position of the "target" digit on the screen (left or right side) was pseudorandomly determined in each sequence repetition, so that only the sequence of digits was structured, not the sequence of motor responses. The two digits were displayed until the participant pressed the response key or for 5000 msec if no response was provided. The participants were asked to respond to the digit presentation as quickly as possible by pressing one response key on a computer keyboard with either the right index or right middle finger. The stimulus–response mapping was always congruent (i.e., the selection of the left digit had to be indicated by an index finger response and that of the right digit by a middle finger response). As soon as the participant provided a response, they received visual feedback for 250 msec: The rectangle border became green when the selected digit belonged to the sequence, whereas a red mask covered the entire rectangle when the response was incorrect (Figure 1C). Then, 500 msec after the keypress or after the 5000-msec limit if no response was provided, the next pair of digits was displayed on the screen. After the completion of one entire sequence (i.e., 16 consecutive trials), a fixation cross appeared again for 2000 msec, indicating the onset of the next sequence.

At the end of the experiment, participants were asked to write down the sequence they learned and explain the strategy they used to memorize it. The appropriate response, if participants used the expected strategy, was 32-32-23-23-41-41-14-14. This test was used a posteriori to select participants who used the anticipated chunking

strategy (excluded participants reported using the 32322-323-41411-414 chunking pattern instead).

Control Task

The participants had to perform the control task once before (CT1) and once after (CT2) the main task. The control task design was the same as that of the main task; that is, the number of items in each sequence (n = 16), the number of sequence repetitions (n = 5), and the trial design were identical. The only differences were as follows: (1) the four digits were replaced by four letters (A, B, C, and D), (2) the two letters displayed simultaneously on the screen were selected at random because there was no sequence to learn, and (3) the target was always the letter B. The aims of this control task were to compare the baseline performance of the two groups and to assess the possible effect of fatigue at the end of the experiment.

TMS

Biphasic TMS pulses were delivered by means of a Magstim Super Rapid stimulator (Magstim Company, Whitland, UK) via a 70-mm-diameter figure-of-eight coil and administered following the cTBS protocol originally described by Huang et al. (2005): Three pulses delivered at 50 Hz every 200 msec for 40 sec, leading to a total of 600 pulses. The stimulation intensity was set at 80% of the resting motor threshold, measured for each participant, in accordance with some earlier studies from our group (Huang & Mouraux, 2015; Zénon, Sidibé, & Olivier, 2015; Torta et al., 2013), as well as others (Chung et al., 2012; Goldsworthy, Pitcher, & Ridding, 2012; Nyffeler et al., 2006). To determine the resting motor threshold, single biphasic pulses were applied over the hand representation of the left primary motor cortex, whereas motor-evoked potentials were recorded from the right first dorsal interosseous muscle. EMG activity was recorded with surface electrodes (Neuroline, Medicotest, Denmark), and the signals were amplified (gain: 1K), band-pass filtered (10–500 Hz; Neurolog Digitimer Ltd., Herefordshire, UK), and digitized online at 1 kHz using a personal computer. Once the optimal position of the coil was found, we determined the minimum intensity needed to produce a 50-μV peak-to-peak motor-evoked potential in 5 of 10 stimulations (Rossini et al., 1994).

cTBS was applied either over left BA 44 (experimental group, n = 12) or the vertex (control group, n = 12). For both stimulation sites, the coil was placed tangentially on the scalp with the handle pointing backward. For the control site (vertex), it was held horizontally and maintained perpendicular to the midsagittal plane; for left BA 44, the coil was pointing with an angle of about 10° upward with respect to the horizontal plane. The coordinates of the targeted stimulation sites were selected from the literature (−46, 10, and 4 mm; x, y, z, Montreal Neurological Institute [MNI] system) for left BA 44 (Heim, Eickhoff, & Amunts, 2009; Amunts et al., 2004) and 0, −15, and 74 mm for the vertex (Okamoto et al., 2004). To position the coil accurately on the scalp surface, the selected target site was located on each individual's structural scan, using a reverse-normalization procedure, and then the coil was guided by means of a homemade neuronavigation system (Davare, Andres, Cosnard, Thonnard, & Olivier, 2006; Zosso et al., 2006; Noirhomme et al., 2004). When required, the coil position was then slightly adjusted to coincide with the "pars opercularis" of the inferior frontal gyrus. At the end of the experiment, we computed the actual coordinates of each individual's TMS site and converted them into the anatomical MNI space (with the anterior commissure as the anatomical reference); for the experimental group, individual TMS sites were superimposed on the probabilistic cytoarchitectonic map gathered for the left BA 44 (Eickhoff et al., 2005, 2007; Figure 2). cTBS was tolerated well by all participants, and no discomfort or other negative side effects were reported.

Data and Statistical Analyses

Five participants (four in the control group and one in the left BA 44 group) of 30 participants were discarded because their chunking strategy differed from that anticipated. An additional control participant was removed from our data set because he executed only 10 correct sequences out of 40, a performance much lower than that of the other participants (correct sequence number: 27.9 ± 5.1, mean ± SD, n = 24). Hence, as mentioned above, the final data set included 24 participants, 12 in each group.

Because the number of correct trials differed between participants, we used generalized linear mixed models (GLMMs) for data analyses. The GLMM approach includes both fixed effects (the predictors or factors of the model) and random effects, taking account of the differences among participants (Baayen, Davidson, & Bates, 2008). The random model was designed considering all within-subject factors and their interactions. As far as the main task was concerned, we performed two separate analyses, one on RT and one on response accuracy. The RT was defined as the delay between the stimulus presentation (digits in the main task and letters in the control task) and the keypress response; RT values were log-transformed to ensure the normality of their distribution (log transformation led to a change in average kurtosis from 15.98 to 3.99 and in skewness from 3.06 to 1.09); incorrect trials and RT values lower than 150 msec were discarded from the analysis. For the second analysis, to determine response accuracy, we computed the ratio between the correct and all the trials; trial-by-trial performance in the task was modeled as a binomial variable. In the models used to analyze RT and accuracy, the predictors

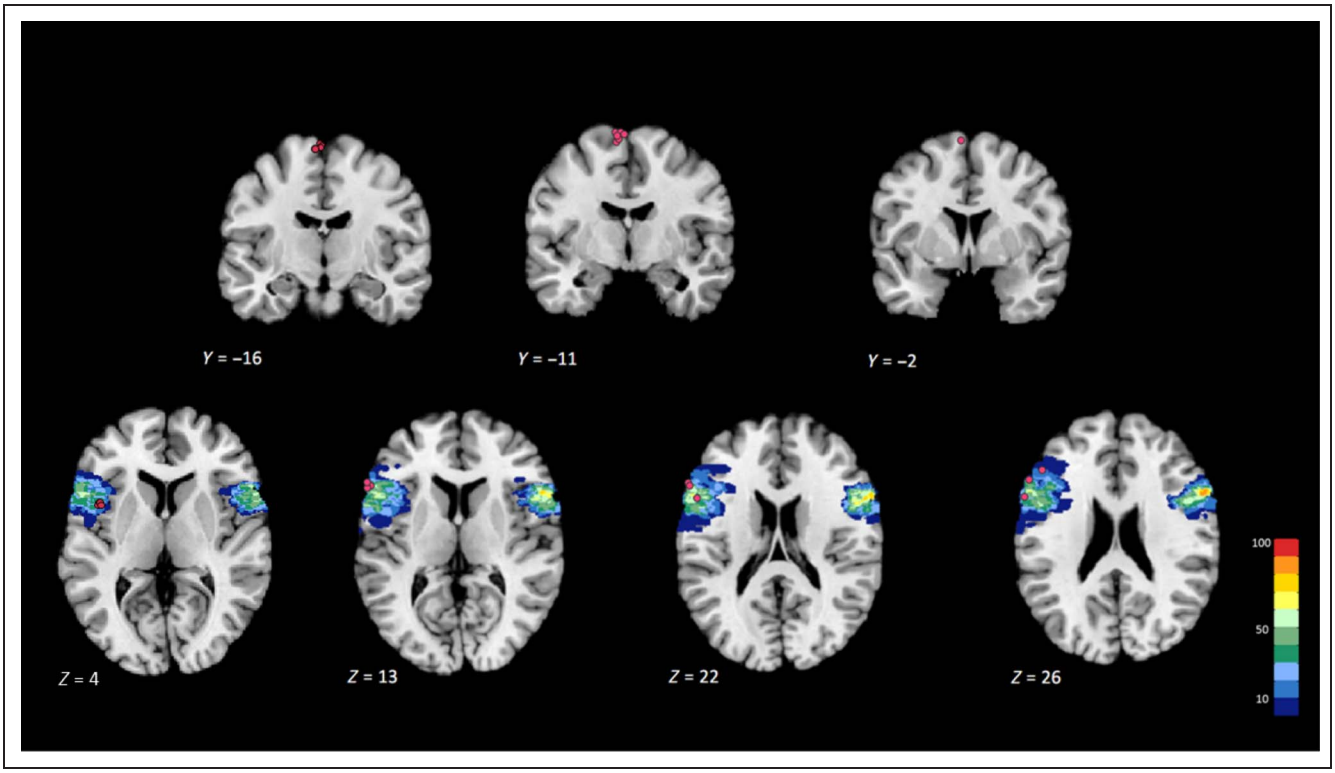

Figure 2. TMS stimulation sites. Upper row: Projection of individual vertex TMS sites (n = 12) on three coronal sections through the MNI single-subject template, at y = −20, −15, and −6, respectively, in anatomical MNI space (+4 in original MNI space). Lower row: Projection of individual left BA 44 TMS sites (n = 12) on four axial sections through the MNI single-subject template, respectively, at z = 9, 18, 27, and 31 in anatomical MNI space (−5 in original MNI space). Probabilistic maps of BA 44 were superimposed on these sections.

taken into account were Group (control vs. left BA 44), Block (from 1 to 8), and Level (Chunking Levels 1, 2, 3, and 4). Because the learning effect followed a decreasing exponential trend, we considered the Block factor as a continuous variable and log-transformed to ensure the linearity between RT and Block and between accuracy and Block; these log transformations increased the log-likelihood of both GLMMs, providing evidence that they improved the model fit.

In addition, to detect baseline difference between the two groups and to evaluate a possible fatigue effect, we analyzed the log-transformed RT gathered in CT1 and CT2 by using a GLMM considering Group (control vs. left BA 44), Block (CT1 vs. CT2), and their interaction as factors. All the analyses were performed using SAS 9.3 software (SAS Institute, Cary, NC).

Finally, to investigate the dynamics of the chunking process on a trial-by-trial basis and its possible change following left BA 44 cTBS, we used a network-based community detection algorithm comparable to that used recently by Grafton and colleagues (Bassett et al., 2013; Wymbs et al., 2012). However, the modularity optimization algorithm we used was slightly different. Indeed, in this study, the modularity function used to detect chunks was influenced by only one parameter, namely the intersequence weight (c1), which allowed us to model the temporal dynamics across sequences (see below for details). This parameter has been set to 0.7, such that the intersequence weight remained comparable to the intrasequence weights (see below for details).

The network-based community detection algorithm we used comprised the following steps:

1. For each participant, each sequence was modeled as a single-layer network (see Figure 3A): The nodes represented each element of the sequence, whereas the weight of the links between each node was defined as follows: $w_{ij} = \frac{\bar{d}_{ij} - d_{ij}}{\bar{d}_{ij}}$, where w_{ij} represents the link between the ith and jth sequence elements, d_{ij} is the difference between the RT for the ith and jth element of the sequence, and $\bar{d}_{ij}$ is the largest d_{ij} value in the sequence. The weight value was bounded between 0 and 1. It is noteworthy that there was only a link between adjacent nodes ($|i - j| = 1$), and therefore, for each sequence, we ended up with a network composed of 16 nodes and 15 links.
2. For each participant, the five sequences belonging to the same block were linked together into a single network, a "block network" that comprised 80 nodes. This network was built by linking each node of the single-layer network with its homologs in the other four sequences; the weights of these links were defined by four distinct constants, as schematically shown in Figure 3A. These four values were linearly dependent and were proportional to c1, the intersequence weight; c2, c3, and c4 were respectively

0.6, 0.45, and 0.3 times c1. These values were selected so that the link between temporally-closer sequences was higher, keeping a balance in the weight distribution; it is noteworthy that small variations of those coefficients did not affect the results of our analysis. This network architecture allowed us to take into account RT changes in neighboring sequences while identifying chunks.

3. Once the block networks were built, we ran a clustering method for each of them, based on modularity optimization (Blondel, Guillaume, Lambiotte, & Lefebvre, 2008). This approach led to the identification of clusters both in the sequence direction (the chunks) and in the orthogonal direction, representing the successive sequences.
4. On the basis of the clusterization performed in the block networks in the previous step, we computed the modularity of each sequence of the block network, named a single-layer network. We thus obtained five values per block network. The modularity was computed using the following formula: $Q = \sum_{ij}[w_{ij} - P_{ij}]\delta(g_i, g_j)$, where w_{ij} is the element ij of the weight matrix of the single-layer network, whereas P_{ij} is the element ij of the weight matrix of the null model (see below); g_i represents the chunk index of the element i, as determined in Step 3; $\delta(g_i, g_j)$ is equal to 1 if $g_i = g_k$, indicating that the elements i and k belong to the same chunk, otherwise it equals 0.

The null model used to compute the modularity in each single-layer network was a matrix whose elements were equal to the node strength, that is, the sum of the weights of each link belonging to a node (Barrat, Barthélemy, Pastor-Satorras, & Vespignani, 2004; Newman & Girvan, 2004). This modularity

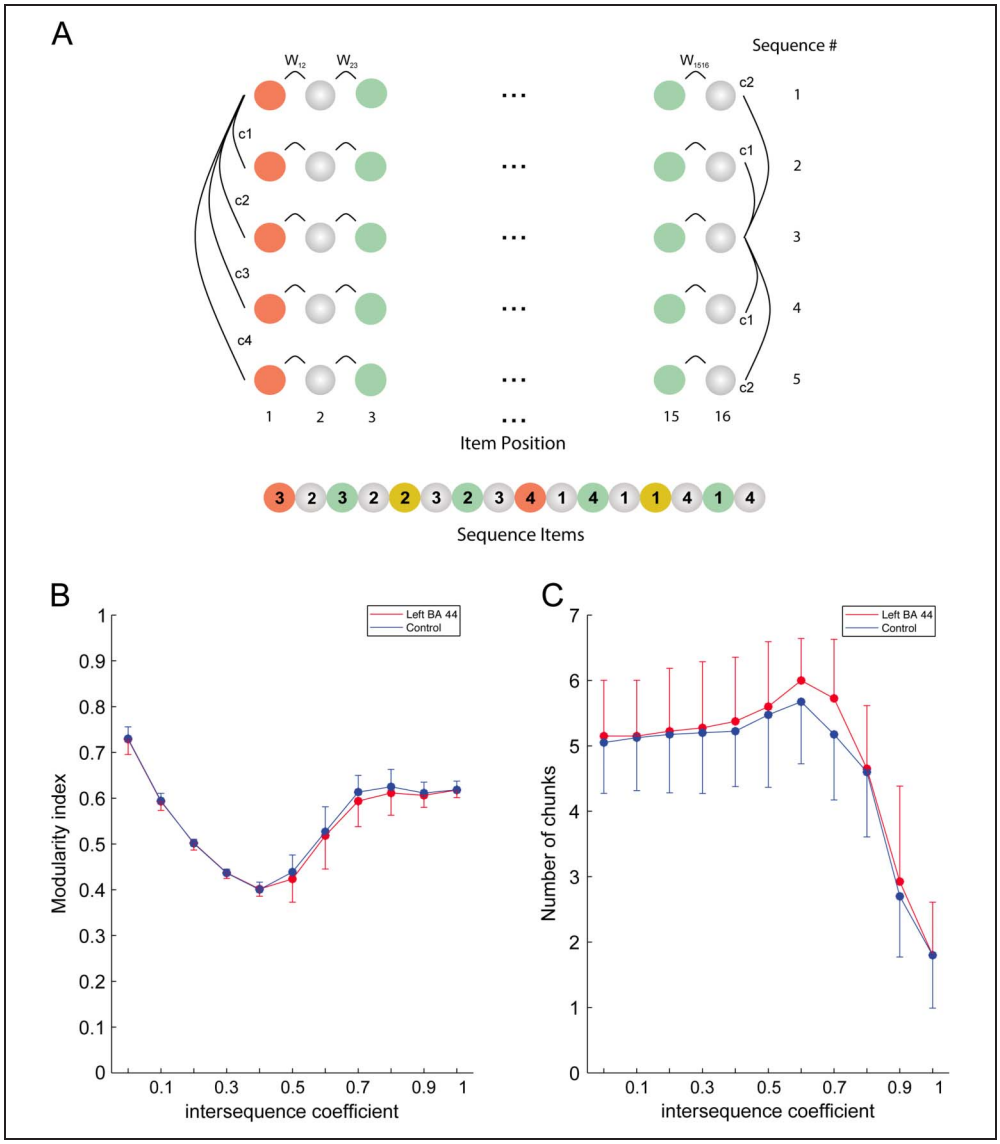

Figure 3. Network-based community detection algorithm. (A) Multisequence network: In the network analysis, each block was modeled by combining the five sequences to constitute a block network. As shown in the figure, only the links between adjacent nodes (W_{ij}, intrasequence weights) and between nodes with the same position in the sequence (c1 to c4, intersequence weights) were considered. The intrasequence weights were computed on the basis of the RTs of each participant (see Methods). The intersequence weights were computed as follows: c2 = 0.6 × c1, c3 = 0.45 × c1 and c4 = 0.3 × c1; c1 was a constant. For illustrative purpose, the intersequence coefficients of the first element of the first row are displayed on the left of the figure (c1, c2, c3, c4), whereas the intersequence coefficients of the last element of the third row are displayed on the right (c1, c2). (B) Change in the modularity index for the left BA 44 (red) and control (blue) groups, when varying the value of intersequence coefficient (c1) by steps of 0.1. Error bars indicate *SD*. (C) Change in the number of chunks for the left BA 44 (red) and control (blue) groups, when varying the value of intersequence coefficient (c1) by steps of 0.1. Error bars indicate *SD*. These figures show that a value of 0.7 (i.e., the value used in remaining analyses) allowed reaching an optimal balance between the number of chunks and modularity index.

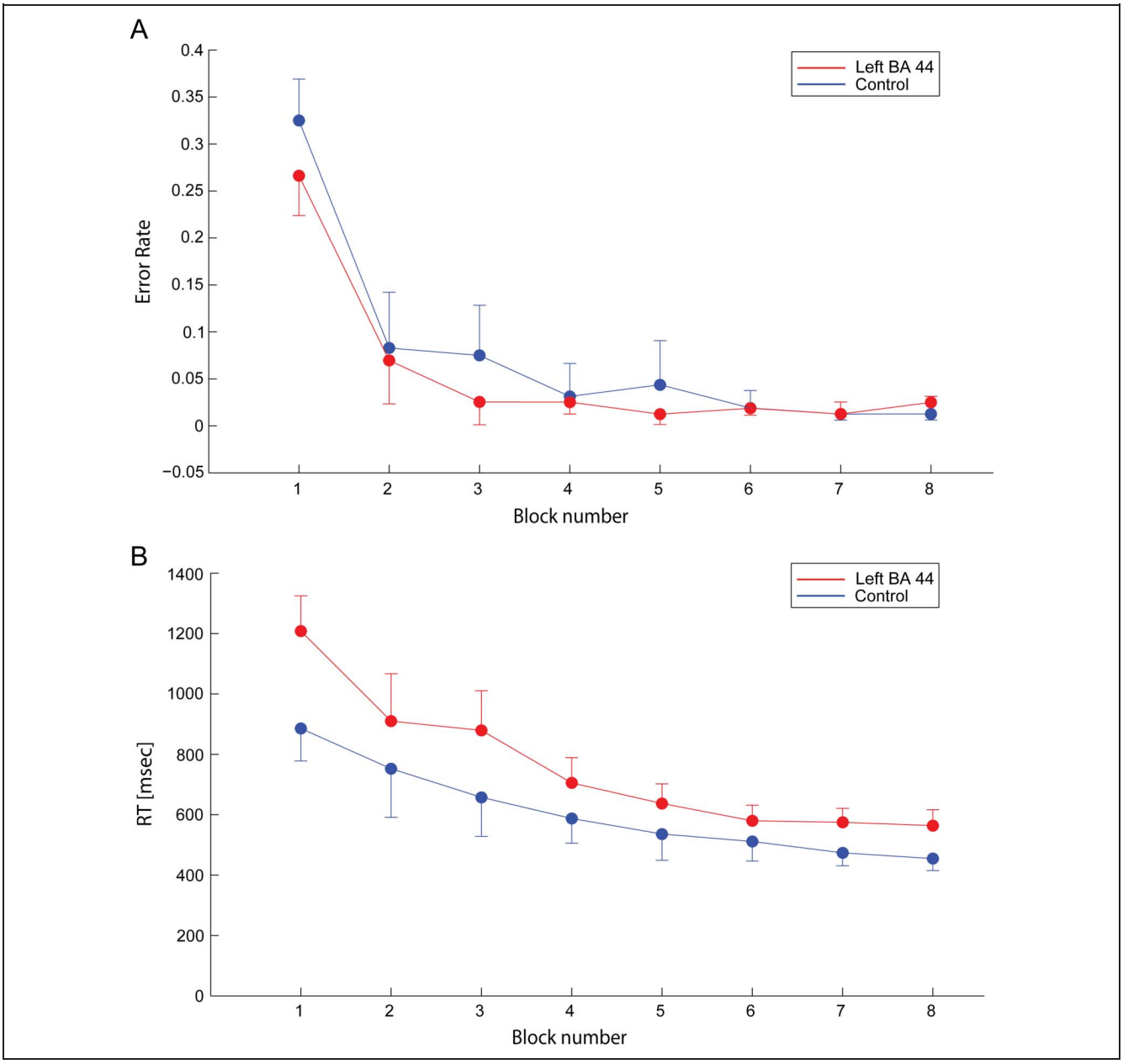

Figure 4. Error rate and RT changes across blocks. (A) Changes in error rate across blocks for the control (blue circles) and left BA 44 (red circles) groups. Error bars indicate *SE*. (B) Decrease in RT across block repetitions for the control (blue circles) and left BA 44 (red circles) groups. Error bars indicate *SE*.

optimization null model is the most commonly used in undirected single-layer networks.

5. In the last step, as proposed by Wymbs et al. (2012), we computed the "chunk magnitude," named φ, which was the reciprocal value of the modularity, gathered for each individual sequence, after having normalized the modularity values for each participant. Wymbs et al. (2012) interpret φ as follows: a low φ value indicates that the community detection algorithm was able to detect chunks easily, suggestive of a high modularity and evocative of what they called the segmentation process, referring to the parsing of the sequence into smaller groups. In contrast, a high φ value indicates that chunks were difficult to isolate, reminiscent of the concatenation process, corresponding to the process of grouping chunks together to build superordinate chunks. Thus, for each participant, we ended up with 40 normalized φ values (5 sequences × 8 blocks) on which we ran a repeated-measures ANOVA with Group and Block as factors. Additionally, to provide a comparison with the results of Wymbs et al. (2012), we computed a linear regression between φ and sequence numbers for each participant. Finally, we fitted a bilinear regression to the

averaged φ values, using least squares estimation (nlinfit function in Matlab) with the following regression function:

$$y = \begin{cases} (ax+b) & if\left(x < \dfrac{e-b}{a-d}\right) \\ (dx+e) & otherwise \end{cases}$$

To evaluate the consistency of our network-based model, we computed the mean modularity for the two groups while varying the intersequence coefficient (c1), the only independent parameter that indicates the strength of the link between the same items across sequences in the block network. This coefficient ranged between 0 (indicating an absence of link between sequences in the block) and 1 (the strongest possible link between successive sequences), with a step of 0.1, for a total of 11 steps. We then followed the same approach for the number of chunks (Figure 3C). For all the following analyses, we selected the value of 0.7, which led to a large modularity index and a relatively large number of chunks (see Figure 3C) and which was close to the average value of the intrasequence coefficients (0.6934 ± 0.0245, mean ± *SE*), allowing to keep the block network balanced across its two dimensions (intrasequence and intersequence). The method we used to determine those parameters fits with the approach followed by Wymbs et al. (2012). This network analysis was implemented by using Matlab (The MathWorks, Inc.).

RESULTS

Control Task

The GLMM analysis performed on the data gathered during the control tasks did not reveal any significant effect neither for the Block factor [$F(1, 22) = 0.12, p = .7319$] nor for the Group factor or the Block × Group interaction [$F(1, 4588) = 1.05, p = .3056$ and $F(1, 4588) = 2.59, p = .1076$, respectively], indicating no significant baseline difference between groups.

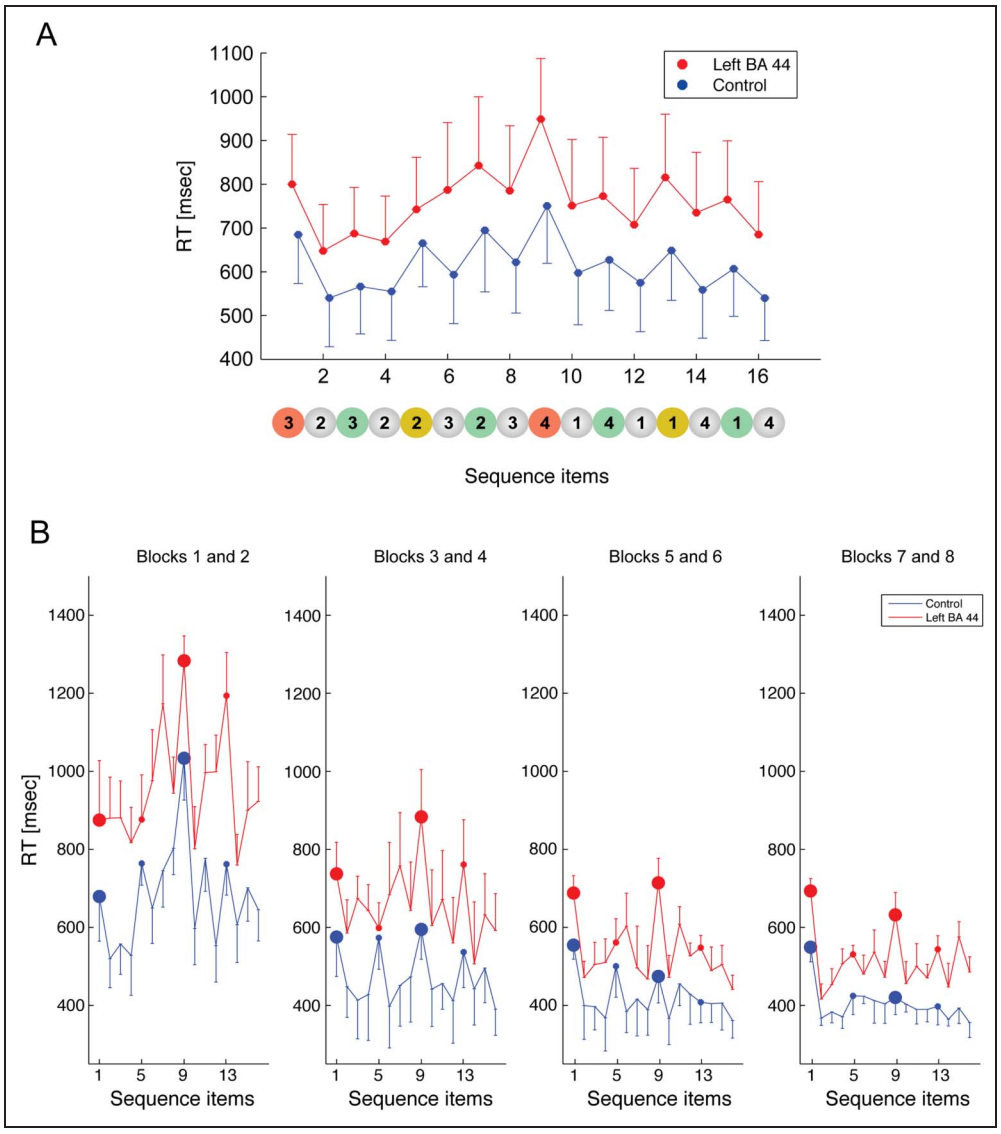

Figure 5. Chunking pattern. (A) RT for each sequence item (from 1 to 16) for all correct sequences in the control (blue lines) and left BA 44 (red lines) groups. Error bars indicate *SE*. (B) RT for each sequence item, as in A, but showing averaged data over pairs of blocks. Large and small dots represent Level 1 and Level 2 items of the sequence, respectively.

Main Task

In the main task, participants had to learn the 16-element sequence during 40 successive repetitions (5 sequences × 8 blocks). We first analyzed the possible influence of left BA 44 TMS on accuracy. A binomial GLMM, considering Block, Group, and Level as factors, indicated a significant Block effect, $F(1, 22) = 294.34, p < .0001$ (see Figure 4A), but no effect of Group, $F(1, 15005) = 1.10, p = .2946$ or of Level, $F(3, 66) = 2.22, p = .0937$; nor were the other interactions significant (all ps $> .05$). It is noteworthy that the Level effect was close to reaching significance, suggesting that the position of a given item in the sequence hierarchy influenced the participants' accuracy, with fewer errors being performed in response to sequence items with the lowest hierarchical level (Level 4 items).

We then examined RT changes across blocks for the two groups to identify the impact of left BA 44 disruption. A GLMM analysis with Group (left BA 44 vs. vertex), Block (Blocks 1–8), and Level (chunk level, from 1 to 4) as fixed effect factors showed a main effect of Block on RT [$F(1, 22) = 107.65, p < .0001$, estimate ± $SE = -0.3266 \pm 0.04098$] but neither a main Group effect, $F(1, 13542) = 2.03, p = .1545$, nor any significant two-way interactions [see Figure 4B, Group × Block: $F(1, 13542) = 0.61, p = .4355$; Block × Level: $F(3, 66) = 0.56, p = .6425$; Level × Group: $F(3, 13542) = 2.07, p = .1021$]. The GLMM analysis also revealed a significant main effect of Level, $F(3, 66) = 13.91, p < .0001$, estimate ± SE: Level 1 = -0.1644 ± 0.03109, Level 2 = -0.01587 ± 0.03088, Level 3 = 0.05912 ± 0.02707, Level 4 = 0.1211 ± 0.02483 (see Figure 1B). Tukey–Kramer adjusted post hoc analyses showed that the main effect of Level resulted from a significant difference between RT for Level 1 items and for the three subsequent levels (all t values > 4.5, all ps $< .0001$) and a significant difference between Levels 2 and 4 (t value = 3.49, $p < .001$) and Levels 3 and 4 (t value = 2.24, $p = .0283$), whereas the comparison between Levels 2 and 3 failed to reach significance ($t = 1.29, p = .2027$). As illustrated in Figure 5, this analysis indicates that the RT to the different items depended on their hierarchical level. Specifically, in both groups, the item position in the sequence affected RT, such that the highest hierarchical levels (Items 1 and 9, Level 1) led to a longer RT. Finally, the three-way interaction was significant [Block × Level × Group, $F(3, 13542) = 3.06, p = .0270$, estimate ± SE for Level 1 = 0.1127 ± 0.03784, Level 2 = -0.04149 ± 0.03768, Level 3 = -0.05139 ± 0.03222, Level 4 = -0.01987 ± 0.02901]. To explore this three-way interaction further, we compared the between-group difference in the slopes of the regression lines computed between RT and blocks across the four hierarchical levels (Figure 6A, B and C). This analysis showed a significant difference only for comparisons between Level 1 and subsequent levels (Levels 1–2: estimate ± $SE = 0.1157 \pm 0.04818, t = 2.40, p = .0164$; Level 1–3: estimate ± $SE = 0.1231 \pm 0.04348, t = 2.83, p = .0046$; Level 1–4: estimate ± $SE = 0.09947 \pm 0.04088, t = 2.43, p = .0150$; all p values Tukey–Kramer corrected); no other comparisons were significant (all ps $> .05$). As illustrated in Figure 6A, for items belonging to Levels 2–4, the computed slopes of the regression lines for each group converged, reducing the distance between the left BA 44 and control groups across block repetition. In contrast, for Level 1 items, the slopes diverged, showing that the distance between the two groups increased across blocks, suggesting a slower improvement for Level 1 items for the left BA 44 group compared with controls. Overall, these results indicate that left BA 44 cTBS altered only the processing of higher-level chunks, leaving unaffected the processing of lower-level chunks.

Finally, to investigate chunking dynamics during learning on a sequence-by-sequence basis and its possible alteration following left BA 44 TMS, we used a network-based community detection algorithm (Bassett et al., 2013; Wymbs et al., 2012) to compute the "chunk magnitude" (φ) for each sequence. As a reminder, a low φ value indicates that the sequence was easily separable into chunks by the community detection algorithm, reminiscent of an ongoing segmentation process, whereas a high φ value indicates that chunks were difficult to isolate, suggesting a concatenation process or the absence of chunks (Wymbs et al., 2012). In a first analysis, we computed the mean φ value for each sequence ($n = 40$), separately for each group (12 participants per group). The variations of φ across sequences were dramatically different between groups (Figure 7). In controls, the mean φ values increased across sequence repetitions (linear regression between average φ and sequence number, slope = 0.001, $p = .03$), in agreement with the finding of Wymbs et al. (2012). In contrast, following cTBS application over left BA 44, we observed a negative slope (linear regression, slope = $-0.0037, p = .02$). Because the linear regression failed to account for the time course of φ across sequences, we also performed a bilinear regression (see Methods). In the BA 44 group, we found a significant negative φ slope in the beginning of the sequence learning (estimate 95% confidence interval [CI]: $-0.0933, -0.02$) and a flat φ function thereafter (estimate CI: $-0.0031, 0.0012$). In the control group, the initial part of the φ function was flat (estimate CI: $-0.0018, 0.0043$), whereas the later portion had a positive slope (estimate CI: 0.0118, 0.0228). Finally, this difference in φ variation between groups was confirmed by performing a two-way, repeated-measures ANOVA on all the φ values ($n = 960$, 24 participants × 8 blocks × 5 sequences/block) with Group and Block as factors. This analysis revealed a main effect of Block ($p < .0001$) and Group ($p = .0216$) and a significant Group × Block interaction ($p < .0001$), confirming that φ was lower in the control group during the first blocks, whereas it decreased in the last blocks in the BA 44 group.

DISCUSSION

This study shows that disruption of Broca's area modifies the processing time of higher-order chunks during the

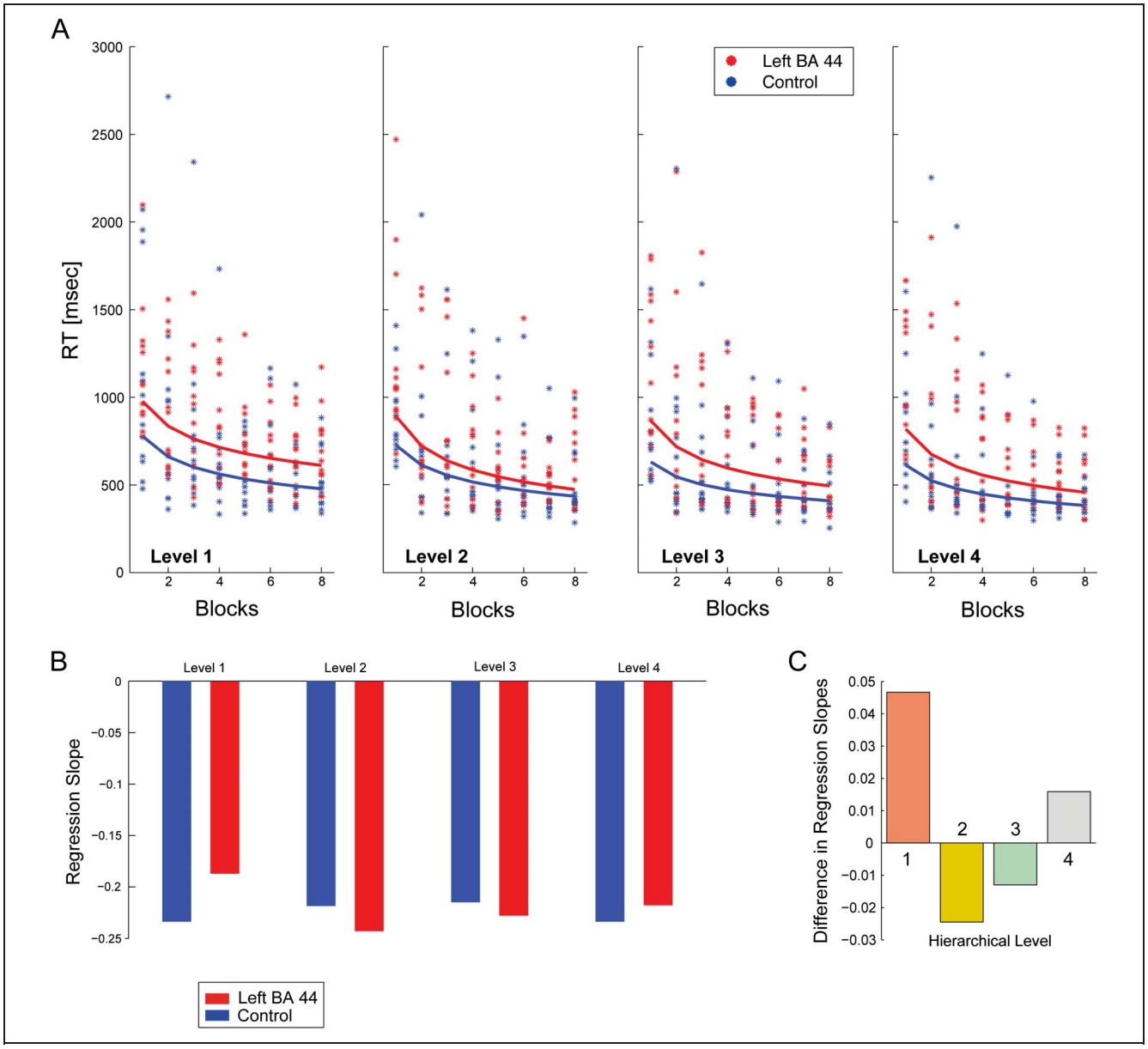

Figure 6. RT change across blocks for items at different chunking levels (from 1 to 4). (A) Each dot represents the average RT for items belonging to the same chunking level, for each participant from either the control (blue dots) or the left BA 44 (red dots) groups, computed for all correct sequences. The BLOCK factor was modeled as a continuous log-transformed variable but displayed on a linear scale. For each chunking level, the regression lines computed between RT and log-transformed block numbers is shown. Only the slopes of the regression lines computed for Level 1 items were significantly different between the two groups when compared with the three other levels. (B) Slope values for each hierarchical level are displayed, in red for the left BA 44 group and in blue for the control group. (C) Slope differences for regression lines computed for each chunking level. Same color convention as in Figure 1.

learning, by trial and error, of a highly structured perceptual sequence, involving neither motor nor explicit linguistic components. cTBS applied over the left BA 44 also changed the dynamics of chunk formation during learning, as demonstrated by the network-based community detection analysis showing that the evolution of the "chunking magnitude" (φ) across sequences is strikingly different following Broca's area disruption.

As already mentioned, the behavioral signature of a chunk is an increased processing time of its first boundary item (Clerget et al., 2012; Pammi et al., 2012; Koechlin & Jubault, 2006; Kennerley, Sakai, & Rushworth, 2004; Rosenbaum et al., 1983), and in a strongly structured hierarchical sequence such as the one used in the current study, this difference in processing times is particularly evident for stimuli occupying higher-level positions, especially Level 1 stimuli. This suggests that the relational patterns in stimulus sequences can elicit low-level chunks, which can be further integrated into superordinate chunks to create a hierarchically organized sequence (Koch & Hoffmann, 2000). In participants learning such a sequence explicitly, we demonstrated that cTBS applied over the

left BA 44 only increases the processing time of stimuli marking the boundaries of superordinate chunks, leaving lower-level chunk processing unchanged, compared with control. This finding corroborates the view that Broca's area plays a critical role in processing sequences (Fitch & Martins, 2014; Opitz & Friederici, 2007; Schubotz & Fiebach, 2006; Tettamanti & Weniger, 2006) and that its contribution is all the more important in hierarchically complex sequences, as previously suggested for both linguistic (Grodzinsky & Santi, 2008; Rogalsky, Matchin, & Hickok, 2008; Santi & Grodzinsky, 2007; Fiebach, Schlesewsky, Lohmann, Von Cramon, & Friederici, 2005) and nonlinguistic tasks (Clerget et al., 2013; Koechlin & Jubault, 2006).

In the current study, it could be argued that cTBS applied over Broca's area interfered with higher-order chunking processing because it requires more cognitive resources, such as increased working memory or executive control demands. Indeed, when processing a higher-order chunk, lower-order items need to be retrieved and held in a buffer. Although a growing number of studies have investigated the possible involvement of Broca's area in working memory in both linguistic and nonlinguistic tasks, a consensus on its role is still lacking. On the one hand, some studies have concluded that Broca's area is involved in language processing via its contribution to working memory (Nee et al., 2013; Rogalsky et al., 2008; Fiebach et al., 2005; Smith, Jonides, & Koeppe, 1996) or via complex interactions between syntactic and working memory processes (Santi & Grodzinsky, 2007; Kaan & Swaab, 2002). Some authors have even suggested that Broca's area implements a "working memory buffer" shared among numerous cognitive systems (including music, action, sequence processing, and language), which could explain its involvement in so many different cognitive tasks (Fitch & Martins, 2014). On the other hand, it is clear that several processes operate on information stored in working memory, namely encoding, maintenance, and retrieval (Jonides et al., 2008), and we are still a long way from fully understanding the contribution, if any, of the frontal cortex and Broca's area in particular to these mechanisms during sequence learning. An important goal for future research will be to investigate the relationship between chunking and working memory, because these two processes might be flip sides of the same coin. Another potential confound in the interpretation of our results is that the participants may have relied on inner speech to maintain the sequence in memory (Baddeley, Gathercole, & Papagno, 1998). Therefore, it could be argued that the disruption of BA 44 impacted the task performance through its effect on language. An argument against this hypothesis is that TMS disruption led to a specific alteration of higher-order chunking performance, whereas it seems that alterations of linguistic processes should have rather disrupted the global sequence learning performance, irrespective of the hierarchical level. In addition, we showed in a previous study that BA 44 disruption led to behavioral alterations in an implicit learning task, in which no inner speech could be involved (Clerget et al.,

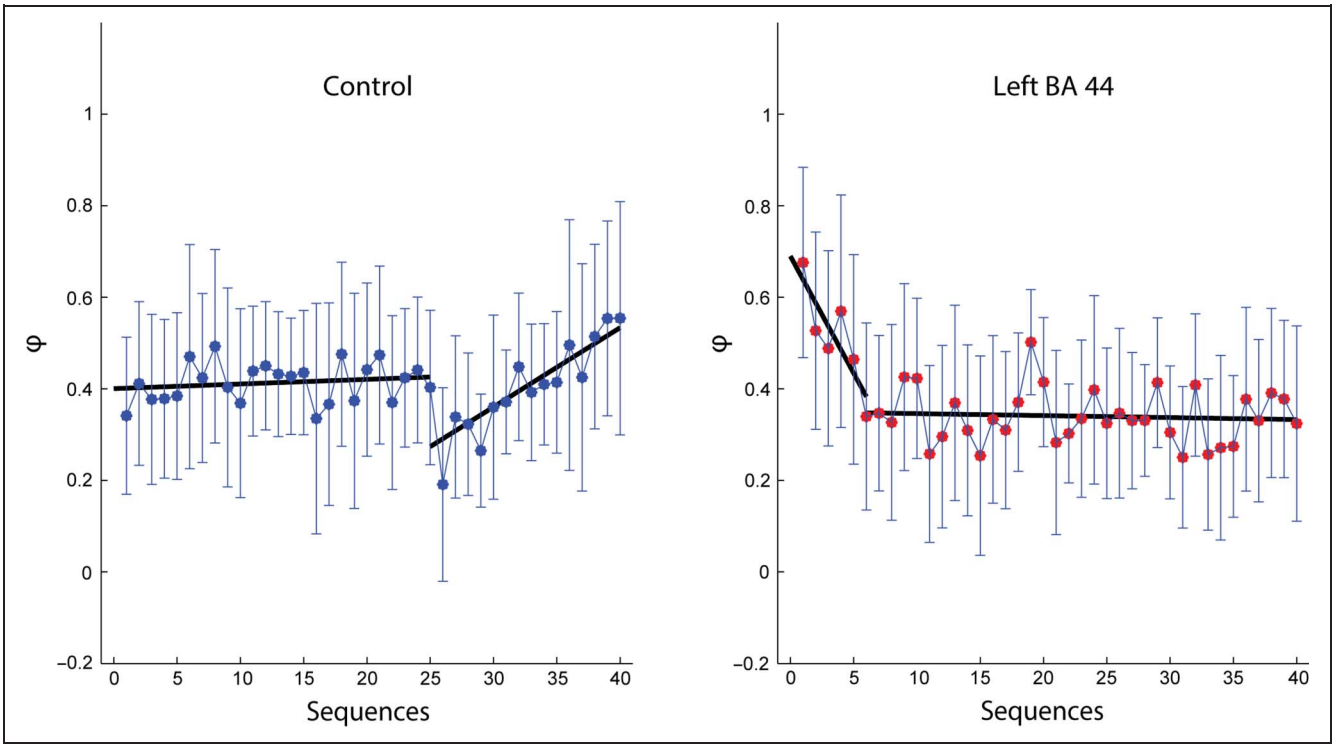

Figure 7. Change in "chunking magnitude" across sequences. The φ values computed for each sequence (1–40) and averaged across participants are shown for the two groups. A bilinear regression was computed for each set of group data. Error bars indicate *SE*.

2012). However, excluding formally this alternative interpretation will require further experiments.

In the current study, the contribution of left BA 44 to chunking was also evidenced by a community detection network analysis, showing that the two groups of participants adopted a strikingly different chunking strategy during sequence learning, as shown by the evolution of the chunking magnitude (φ) across sequences. In the control group, we found, in accordance with the work of Grafton and colleagues (Wymbs et al., 2012), that φ increases gradually during sequence learning. In the framework of motor sequence learning, chunking has been theorized as a twofold dynamic process, relying on distinct mechanisms. The first chunking operation, called "segmentation," leads to the parsing of the sequence into shorter clusters or "chunks" (Wymbs et al., 2012; Sakai et al., 2003; Verwey & Eikelboom, 2003; Verwey, 2001; Koch & Hoffmann, 2000) and is characterized by a high modularity and therefore by a low φ value (Wymbs et al., 2012). The second chunking process, the "concatenation," occurs probably at a later stage of learning and consists of integrating those elementary chunks into superordinate chunks (Wymbs et al., 2012; Sakai et al., 2003; Koch & Hoffmann, 2000; Verwey, 1996), leading to a decrease in modularity, revealed by a higher φ value (Wymbs et al., 2012). The progressive φ increase we observed in our control participants can thus be construed as evidence for a gradual occurrence of concatenation, although we found that φ did not increase monotonically across sequences as reported originally (Wymbs et al., 2012), but rather was augmented abruptly in the second half of the training session, possibly corresponding to the moment when the participants reached a plateau in terms of both error and RT (see Figure 4). Interestingly, we found that left BA 44 cTBS altered the φ change across sequence repetitions (see Figure 7): first, cTBS yielded a much higher φ value than in controls at the beginning of the training session, followed by a rapid decrease during the first half of the experiment; second, φ values remained more or less constant (or were even slightly decreased) during the second half of the training session. To understand this chunking strategy, it is important to keep in mind that a high φ value suggests a difficulty for the community detection algorithm in isolating chunks, and although a high φ value at the end of training has been regarded as evidence for concatenation (see above), it could also be explained by a lack of or a very low number of chunks in the sequence. Our interpretation is that following BA 44 disruption, the whole progression of the chunking processing was delayed, with segmentation occurring later and concatenation failing to happen within the time frame of the experiment. Alternatively, it could be proposed that the delayed pattern of φ change across blocks in the BA 44 group was caused by a disruption of learning rather than chunking specifically. The observation that RT alterations were level specific argues strongly against this hypothesis. However, it must be pointed out that our task was designed to highlight the role of BA 44 in chunking specifically and was very easy to learn. Therefore, we cannot exclude that this region may be important in other, more global, aspects of sequence learning, as shown in a previous study (Clerget et al., 2012). Finally, it is noteworthy that one limit of the model used in the current study is that it assumes a constant intersequence weight, whereas in fact it is likely to increase over time. More complex models, accounting for these changes over time, have been proposed recently (Mucha, Richardson, Macon, Porter, & Onnela, 2010). However, given that, in the present task, the sequences were learned very quickly, we believe that using such a model would not impact significantly on our results.

Regarding the neural correlates of chunking, although many functional imaging studies have sought to identify structures involved in sequence learning (Ashe et al., 2006; Rhodes, Bullock, Verwey, Averbeck, & Page, 2004; Grafton, Hazeltine, & Ivry, 1998; Toni, Krams, Turner, & Passingham, 1998), only very few studies have explicitly tried to identify the neural correlates of chunking (Ruitenberg, Verwey, Schutter, & Abrahamse, 2014; Pammi et al., 2012; Wymbs et al., 2012; Kennerley et al., 2004; Verwey, Lammens, & van Honk, 2002). An exception is the BG, for which a contribution to chunking has already been demonstrated (Wymbs et al., 2012; Tremblay et al., 2010; Boyd et al., 2009; Tanji, 2001; Graybiel, 1998). As far as the involvement of cortical areas in chunking is concerned, in a recent functional imaging study Pammi and colleagues investigated the effect of sequence complexity on the BOLD signal in a frontoparietal network, including the VLPFC, and tried to relate these changes to chunking (Pammi et al., 2012). Increasing the sequence complexity led, in the early stages, to a larger activation in bilateral VLPFC, including BA 44 and BA 45. Then, in the intermediate learning stage, this activation moved leftward and more dorsally to the dorsolateral pFC. Because this increase in sequence complexity was also accompanied by the emergence of chunking, the authors speculated that these changes in BOLD signals in VLPFC might be related to the encoding and execution of chunks (Pammi et al., 2012). Moreover, Wymbs and colleagues interpreted the negative correlation that they found between φ and the BOLD signal in the left frontoparietal network, including the left inferior frontal sulcus, as evidence for its involvement in chunk segmentation, contrasting with the positive correlation between φ and activation of the bilateral sensorimotor putamen, interpreted as illustrative of its involvement in concatenation (Wymbs et al., 2012). This study certainly implicates the left inferior frontal gyrus in the chunking process but does not allow us to isolate clearly its specific contribution to either segmentation or concatenation. On the basis of the time course of φ following cTBS, it seems that left BA 44 disruption delayed the sequence segmentation, and prevented further concatenation. One possible explanation is that concatenation did not occur in this study because of delayed segmentation, the experiment duration being

too short to see the emergence of concatenation. The difficulty in reconciling these results illustrates the limitations inherent in the decryption of the neural correlates of the chunking process with functional neuroimaging techniques because of the fluctuating contribution of different brain structures during training (Pammi et al., 2012; Bassett et al., 2011; Bapi, Miyapuram, Graydon, & Doya, 2006; Sakai et al., 1998) and because chunking is, by definition, a dynamic process (Clerget et al., 2012; Pammi et al., 2012), which is generally highly variable between subjects (Wymbs et al., 2012; Kennerley et al., 2004). Moreover, it is likely that segmentation and concatenation are parallel processes overlapping in time during learning, making it even more difficult to disentangle them and to pinpoint their respective neural correlates using functional MRI.

Despite decades of research, the role of Broca's area is still unclear and remains a source of debate. Indeed, the finding that Broca's area is involved in so many different cognitive functions (Fitch & Martins, 2014; Clos, Amunts, Laird, Fox, & Eickhoff, 2013; Fedorenko, Duncan, & Kanwisher, 2012; Fadiga, Craighero, & D'Ausilio, 2009; Grodzinsky & Santi, 2008; Nishitani, Schürmann, Amunts, & Hari, 2005) has been seen as an argument for the view that it implements a general, effector-independent mechanism such as working memory, hierarchy, syntactic processing, or possibly cognitive control. In contrast, the contribution of Broca's area to such a wide range of cognitive tasks might imply functional heterogeneity and its parcellation into specialized subregions (Fedorenko et al., 2012), a view substantiated by a recent study of the anatomical segregation of BA 44 and 45 (Amunts et al., 2010). Our finding that Broca's area plays a role in processing higher-order chunks, supports the "broad-spectrum mechanism" hypothesis, and is reminiscent of the conclusions of Koechlin and Jubault (2006), who proposed a model in which the anterior (BA 45) and posterior (BA 44) parts of Broca's area—and of its right homolog—constitute, with the dorsal premotor cortex (BA 6), a rostrocaudally organized network for processing hierarchically structured sequences. One key conclusion of that study was that motor behavior shares some similarities with language and that a complex action can be viewed as a chain of subordinate movements, which need to be combined according to certain rules to reach a given goal (Botvinick, 2008; Dominey et al., 2003; Dehaene & Changeux, 1997). Sequence learning in particular appears to rely on cognitive processes that are shared with language (Granena, 2013; Nemeth et al., 2011; Conway, Karpicke, & Pisoni, 2007). On the basis of the results of the current study, it is tempting to hypothesize that Broca's area could be involved in higher-order chunk processing whenever a serial stream of information has to be processed (Pallier, Devauchelle, & Dehaene, 2011; Bapi, Doya, & Harner, 2000). Moreover, because many studies on perception, learning, and cognition support the view that chunking is a universal information-processing mechanism (Kurby & Zacks, 2008; Gobet et al., 2001), it is tempting to hypothesize that chunking is a basic mechanism that makes Broca's area central to a large number of different cognitive and sensorimotor domains. Verifying the validity of this assumption will require further experiments to prove that left BA 44 cTBS alters higher-order chunking in tasks from different domains.

As already mentioned, besides Broca's area, the other structure commonly considered to be involved in chunking is the BG (Jin, Tecuapetla, & Costa, 2014; Wymbs et al., 2012; Boyd et al., 2009; Graybiel, 1998). Interestingly, in addition to their well-known contribution to motor sequence processing, BGs are also involved in language syntax (Ackermann, Hage, & Ziegler, 2014; Chan, Ryan, & Bever, 2013; Vargha-Khadem, Gadian, Copp, & Mishkin, 2005; Watkins & Dronkers, 2002; Alcock, Passingham, Watkins, & Vargha-Khadem, 2000) and working memory (Cools, 2011; Cools & D'Esposito, 2011; Baier et al., 2010), a combination of functions strikingly similar to those assigned to Broca's area. Details are still lacking on how Broca's area interacts with the BG (Ullman, 2006), but this further highlights the possible connections between working memory, syntax, and chunking (Zénon & Olivier, 2014). It also emphasizes the tight interaction between action-related and higher cognitive functions (Mendoza & Merchant, 2014; Andres, Olivier, & Badets, 2008; Olivier, Davare, Andres, & Fadiga, 2007), supporting the view that the latter have invaded evolutionarily older motor brain circuits during the course of evolution (Dehaene & Cohen, 2007).

Acknowledgments

This work was performed at the Institute of Neuroscience of the Université catholique de Louvain (Brussels, Belgium); it was supported by grants from the ARC (Actions de Recherche Concertées, Communauté Française de Belgique), the Fondation Médicale Reine Elisabeth (FMRE), and the Fonds de la Recherche Scientifique (FNRS-FDP) to E. O., by EU grants Poeticon++ and Siempre, and by the E.R. Region-University fund to L. F. A. A. is a Research Fellow at the FNRS and A. Z. is a Senior Research Associate supported by INNOVIRIS. The authors appreciate the assistance of Emeline Clerget in running some subjects. We are also grateful to Benvenuto Jacob for his help in programming, to Laurence Dricot for processing the TMS site locations, and to Vincent Blondel for his advice on data analysis.

Reprint requests should be sent to Prof. Etienne Olivier, Institute of Neuroscience, Université catholique de Louvain, 53, Avenue Mounier, COSY-B1.53.04, 1200 Brussels, Belgium, or via e-mail: etienne.olivier@uclouvain.be.

REFERENCES

Ackermann, H., Hage, S. R., & Ziegler, W. (2014). Brain mechanisms of acoustic communication in humans and nonhuman primates: An evolutionary perspective. *Behavioral and Brain Sciences, 37,* 1–84.

Alcock, K. J., Passingham, R. E., Watkins, K. E., & Vargha-Khadem, F. (2000). Oral dyspraxia in inherited speech and language impairment and acquired dysphasia. *Brain and Language, 75,* 17–33.

Amunts, K., Lenzen, M., Friederici, A. D., Schleicher, A., Morosan, P., Palomero-Gallagher, N., et al. (2010). Broca's region: Novel organizational principles and multiple receptor mapping. *PLoS Biology, 8,* e1000489.

Amunts, K., Weiss, P. H., Mohlberg, H., Pieperhoff, P., Eickhoff, S., Gurd, J. M., et al. (2004). Analysis of neural mechanisms underlying verbal fluency in cytoarchitectonically defined stereotaxic space—The roles of Brodmann areas 44 and 45. *Neuroimage, 22,* 42–56.

Andres, M., Olivier, E., & Badets, A. (2008). Actions, words, and numbers: A motor contribution to semantic processing? *Current Directions in Psychological Science, 17,* 313–317.

Ashe, J., Lungu, O. V., Basford, A. T., & Lu, X. (2006). Cortical control of motor sequences. *Current Opinion in Neurobiology, 16,* 213–221.

Baayen, R. H., Davidson, D. J., & Bates, D. M. (2008). Mixed-effects modeling with crossed random effects for subjects and items. *Journal of Memory and Language, 59,* 390–412.

Baddeley, A., Gathercole, S., & Papagno, C. (1998). The phonological loop as a language learning device. *Psychological Review, 105,* 158–173.

Bahlmann, J., Schubotz, R. I., Mueller, J. L., Koester, D., & Friederici, A. D. (2009). Neural circuits of hierarchical visuo-spatial sequence processing. *Brain Research, 1298,* 161–170.

Baier, B., Karnath, H.-O., Dieterich, M., Birklein, F., Heinze, C., & Müller, N. G. (2010). Keeping memory clear and stable—The contribution of human basal ganglia and prefrontal cortex to working memory. *Journal of Neuroscience, 30,* 9788–9792.

Bapi, R. S., Doya, K., & Harner, A. M. (2000). Evidence for effector independent and dependent representations and their differential time course of acquisition during motor sequence learning. *Experimental Brain Research, 132,* 149–162.

Bapi, R. S., Miyapuram, K. P., Graydon, F. X., & Doya, K. (2006). fMRI investigation of cortical and subcortical networks in the learning of abstract and effector-specific representations of motor sequences. *Neuroimage, 32,* 714–727.

Barrat, A., Barthélemy, M., Pastor-Satorras, R., & Vespignani, A. (2004). The architecture of complex weighted networks. *Proceedings of the National Academy of Sciences, U.S.A., 101,* 3747–3752.

Bassett, D. S., Porter, M. A., Wymbs, N. F., Grafton, S. T., Carlson, J. M., & Mucha, P. J. (2013). Robust detection of dynamic community structure in networks. *Chaos, 23,* 1–16.

Bassett, D. S., Wymbs, N. F., Porter, M. A., Mucha, P. J., Carlson, J. M., & Grafton, S. T. (2011). Dynamic reconfiguration of human brain networks during learning. *Proceedings of the National Academy of Sciences, U.S.A., 108,* 7641–7646.

Blondel, V. D., Guillaume, J.-L., Lambiotte, R., & Lefebvre, E. (2008). Fast unfolding of communities in large networks. *Journal of Statistical Mechanics: Theory and Experiment,* P10008. doi:10.1088/1742-5468/2008/10/P10008.

Bor, D., Duncan, J., Wiseman, R. J., & Owen, A. M. (2003). Encoding strategies dissociate prefrontal activity from working memory demand. *Neuron, 37,* 361–367.

Bor, D., & Seth, A. K. (2012). Consciousness and the prefrontal parietal network: Insights from attention, working memory, and chunking. *Frontiers in Psychology, 3,* 1–14.

Botvinick, M. M. (2008). Hierarchical models of behavior and prefrontal function. *Trends in Cognitive Sciences, 12,* 201–208.

Boyd, L. A., Edwards, J. D., Siengsukon, C. S., Vidoni, E. D., Wessel, B. D., & Linsdell, M. A. (2009). Motor sequence chunking is impaired by basal ganglia stroke. *Neurobiology of Learning and Memory, 92,* 35–44.

Chan, S.-H., Ryan, L., & Bever, T. G. (2013). Role of the striatum in language: Syntactic and conceptual sequencing. *Brain and Language, 125,* 283–294.

Chung, H.-K., Tsai, C.-H., Lin, Y.-C., Chen, J.-M., Tsou, Y.-A., Wang, C.-Y., et al. (2012). Effectiveness of theta-burst repetitive transcranial magnetic stimulation for treating chronic tinnitus. *Audiology & Neuro-Otology, 17,* 112–120.

Clerget, E., Andres, M., & Olivier, E. (2013). Deficit in complex sequence processing after a virtual lesion of left BA 45. *PLoS One, 8,* 1–9.

Clerget, E., Badets, A., Duqué, J., & Olivier, E. (2011). Role of Broca's area in motor sequence programming: A cTBS study. *NeuroReport, 22,* 965–969.

Clerget, E., Poncin, W., Fadiga, L., & Olivier, E. (2012). Role of Broca's area in implicit motor skill learning: Evidence from continuous theta-burst magnetic stimulation. *Journal of Cognitive Neuroscience, 24,* 80–92.

Clerget, E., Winderickx, A., Fadiga, L., & Olivier, E. (2009). Role of Broca's area in encoding sequential human actions: A virtual lesion study. *NeuroReport, 20,* 1496–1499.

Clos, M., Amunts, K., Laird, A. R., Fox, P. T., & Eickhoff, S. B. (2013). Tackling the multifunctional nature of Broca's region meta-analytically: Co-activation-based parcellation of area 44. *Neuroimage, 83,* 174–188.

Conway, C. M., & Christiansen, M. H. (2001). Sequential learning in non-human primates learning fixed sequences. *Trends in Cognitive Sciences, 5,* 539–546.

Conway, C. M., Karpicke, J., & Pisoni, D. B. (2007). Contribution of implicit sequence learning to spoken language processing: Some preliminary findings with hearing adults. *Journal of Deaf Studies and Deaf Education, 12,* 317–334.

Cools, R. (2011). Dopaminergic control of the striatum for high-level cognition. *Current Opinion in Neurobiology, 21,* 402–407.

Cools, R., & D'Esposito, M. (2011). Inverted-U-shaped dopamine actions on human working memory and cognitive control. *Biological Psychiatry, 69,* e113–e125.

Corballis, M. C. (2003). From mouth to hand: Gesture, speech, and the evolution of right-handedness. *Behavioral and Brain Sciences, 26,* 199–208; discussion 208–260.

Davare, M., Andres, M., Cosnard, G., Thonnard, J.-L., & Olivier, E. (2006). Dissociating the role of ventral and dorsal premotor cortex in precision grasping. *Journal of Neuroscience, 26,* 2260–2268.

Dehaene, S., & Changeux, J. P. (1997). A hierarchical neuronal network for planning behavior. *Proceedings of the National Academy of Sciences, U.S.A., 94,* 13293–13298.

Dehaene, S., & Cohen, L. (2007). Cultural recycling of cortical maps. *Neuron, 56,* 384–398.

Dominey, P. F., Hoen, M., Blanc, J. M., & Lelekov-Boissard, T. (2003). Neurological basis of language and sequential cognition: Evidence from simulation, aphasia, and ERP studies. *Brain and Language, 86,* 207–225.

Doyon, J., Bellec, P., Amsel, R., Penhune, V., Monchi, O., Carrier, J., et al. (2009). Contributions of the basal ganglia and functionally related brain structures to motor learning. *Behavioural Brain Research, 199,* 61–75.

Eickhoff, S. B., Paus, T., Caspers, S., Grosbras, M. H., Evans, A. C., Zilles, K., et al. (2007). Assignment of functional activations to probabilistic cytoarchitectonic areas revisited. *Neuroimage, 36,* 511–521.

Eickhoff, S. B., Stephan, K. E., Mohlberg, H., Grefkes, C., Fink, G. R., Amunts, K., et al. (2005). A new SPM toolbox for combining probabilistic cytoarchitectonic maps and functional imaging data. *Neuroimage, 25,* 1325–1335.

Fadiga, L., Craighero, L., & D'Ausilio, A. (2009). Broca's area in language, action, and music. *Annals of the New York Academy of Sciences, 1169,* 448–458.

Fazio, P., Cantagallo, A., Craighero, L., D'Ausilio, A., Roy, A. C., Pozzo, T., et al. (2009). Encoding of human action in Broca's area. *Brain, 132,* 1980–1988.
Fedorenko, E., Duncan, J., & Kanwisher, N. (2012). Language-selective and domain-general regions lie side by side within Broca's area. *Current Biology, 22,* 2059–2062.
Fiebach, C. J., Schlesewsky, M., Lohmann, G., Von Cramon, D. Y., & Friederici, A. D. (2005). Revisiting the role of Broca's area in sentence processing: Syntactic integration versus syntactic working memory. *Human Brain Mapping, 24,* 79–91.
Fitch, W. T., & Martins, M. D. (2014). Hierarchical processing in music, language, and action: Lashley revisited. *Annals of the New York Academy of Sciences, 1316,* 87–104.
Gobet, F., Lane, P. C. R., Croker, S., Cheng, P. C., Jones, G., Oliver, I., et al. (2001). Chunking mechanisms in human learning, *Trends in Cognitive Sciences, 5,* 236–243.
Goldsworthy, M. R., Pitcher, J. B., & Ridding, M. C. (2012). A comparison of two different continuous theta burst stimulation paradigms applied to the human primary motor cortex. *Clinical Neurophysiology, 123,* 2256–2263.
Grafton, S. T., Hazeltine, E., & Ivry, R. B. (1998). Abstract and effector-specific representations of motor sequences identified with PET. *Journal of Neuroscience, 18,* 9420–9428.
Granena, G. (2013). Individual differences in sequence learning ability and second language acquisition in early childhood and adulthood. *Language Learning, 63,* 665–703.
Graybiel, A. M. (1998). The basal ganglia and chunking of action repertoires. *Neurobiology of Learning and Memory, 136,* 119–136.
Grodzinsky, Y., & Santi, A. (2008). The battle for Broca's region. *Trends in Cognitive Sciences, 12,* 474–480.
Grossman, M. (1980). A central processor for hierarchically-structured material: Evidence from Broca's aphasia. *Neuropsychologia, 18,* 299–308.
Heim, S., Eickhoff, S. B., & Amunts, K. (2009). Different roles of cytoarchitectonic BA 44 and BA 45 in phonological and semantic verbal fluency as revealed by dynamic causal modelling. *Neuroimage, 48,* 616–624.
Hikosaka, O., Nakamura, K., Sakai, K., & Nakahara, H. (2002). Central mechanisms of motor skill learning. *Current Opinion in Neurobiology, 12,* 217–222.
Huang, G., & Mouraux, A. (2015). MEP latencies predict the neuromodulatory effect of cTBS delivered to the ipsilateral and contralateral sensorimotor cortex. *Plos One, 10,* e0133893.
Huang, Y. Z., Edwards, M. J., Rounis, E., Bhatia, K. P., & Rothwell, J. C. (2005). Theta burst stimulation of the human motor cortex. *Neuron, 45,* 201–206.
Huntley, J., Bor, D., Hampshire, A., Owen, A., & Howard, R. (2011). Working memory task performance and chunking in early Alzheimer's disease. *British Journal of Psychiatry, 198,* 398–403.
Janata, P., & Grafton, S. T. (2003). Swinging in the brain: Shared neural substrates for behaviors related to sequencing and music. *Nature Neuroscience, 6,* 682–687.
Jin, X., Tecuapetla, F., & Costa, R. M. (2014). Basal ganglia subcircuits distinctively encode the parsing and concatenation of action sequences. *Nature Neuroscience, 17,* 423–430.
Jonides, J., Lewis, R. L., Nee, D. E., Lustig, C. A., Berman, M. G., & Moore, K. S. (2008). The mind and brain of short-term memory. *Annual Review of Psychology, 59,* 193–224.
Kaan, E., & Swaab, T. Y. (2002). The brain circuitry of syntactic comprehension. *Trends in Cognitive Sciences, 6,* 350–356.
Keel, J. C., Smith, M. J., & Wassermann, E. M. (2001). A safety screening questionnaire for transcranial magnetic stimulation. *Clinical Neurophysiology, 112,* 720.
Keele, S. W., Ivry, R., Mayr, U., Hazeltine, E., & Heuer, H. (2003). The cognitive and neural architecture of sequence representation. *Psychological Review, 110,* 316–339.
Kennerley, S. W., Sakai, K., & Rushworth, M. F. S. (2004). Organization of action sequences and the role of the pre-SMA. *Journal of Neurophysiology, 91,* 978–993.
Koch, I., & Hoffmann, J. (2000). Patterns, chunks, and hierarchies in serial reaction-time tasks. *Psychological Research, 63,* 22–35.
Koechlin, E., & Jubault, T. (2006). Broca's area and the hierarchical organization of human behavior. *Neuron, 50,* 963–974.
Kühn, A. (2011). *Neuronale Korrelate der Vorhersage hierarchischer Stimulussequenzen*. Rheinisch-Westfälischen Technischen Hochschule Aachen.
Kurby, C. A., & Zacks, J. M. (2008). Segmentation in the perception and memory of events. *Trends in Cognitive Sciences, 12,* 72–79.
Mathy, F., & Feldman, J. (2012). What's magic about magic numbers? Chunking and data compression in short-term memory. *Cognition, 122,* 346–362.
Mendoza, G., & Merchant, H. (2014). Motor system evolution and the emergence of high cognitive functions. *Progress in Neurobiology, 122,* 73–93.
Mucha, P. J., Richardson, T., Macon, K., Porter, M. A., & Onnela, J.-P. (2010). Community structure in time-dependent, multiscale, and multiplex networks. *Science, 328,* 876–879.
Nee, D. E., Brown, J. W., Askren, M. K., Berman, M. G., Demiralp, E., Krawitz, A., et al. (2013). A meta-analysis of executive components of working memory. *Cerebral Cortex, 23,* 264–282.
Nemeth, D., Janacsek, K., Csifcsak, G., Szvoboda, G., Howard, J. H., & Howard, D. V. (2011). Interference between sentence processing and probabilistic implicit sequence learning. *PLoS One, 6,* 6–11.
Newman, M., & Girvan, M. (2004). Finding and evaluating community structure in networks. *Physical Review E, 69,* 026113.
Nishitani, N., Schürmann, M., Amunts, K., & Hari, R. (2005). Broca's region: From action to language. *Physiology, 20,* 60–69.
Noirhomme, Q., Ferrant, M., Vandermeeren, Y., Olivier, E., Macq, B., & Cuisenaire, O. (2004). Registration and real-time visualization of transcranial magnetic stimulation with 3-D MR images. *IEEE Transactions on Bio-Medical Engineering, 51,* 1994–2005.
Nyffeler, T., Wurtz, P., Lüscher, H. R., Hess, C. W., Senn, W., Pflugshaupt, T., et al. (2006). Repetitive TMS over the human oculomotor cortex: Comparison of 1-Hz and theta burst stimulation. *Neuroscience Letters, 409,* 57–60.
Okamoto, M., Dan, H., Sakamoto, K., Takeo, K., Shimizu, K., Kohno, S., et al. (2004). Three-dimensional probabilistic anatomical cranio-cerebral correlation via the international 10-20 system oriented for transcranial functional brain mapping. *Neuroimage, 21,* 99–111.
Oldfield, R. C. (1971). The assessment and analysis of handedness: The Edinburgh inventory. *Neuropsychologia, 9,* 97–113.
Olivier, E., Davare, M., Andres, M., & Fadiga, L. (2007). Precision grasping in humans: From motor control to cognition. *Current Opinion in Neurobiology, 17,* 644–648.
Opitz, B., & Friederici, A. D. (2007). Neural basis of processing sequential and hierarchical syntactic structures. *Human Brain Mapping, 28,* 585–592.
Pallier, C., Devauchelle, A.-D., & Dehaene, S. (2011). Cortical representation of the constituent structure of sentences. *Proceedings of the National Academy of Sciences, U.S.A., 108,* 2522–2527.

Pammi, V. S. C., Miyapuram, K. P., Ahmed, Samejima, K., Bapi, R. S., & Doya, K. (2012). Changing the structure of complex visuo-motor sequences selectively activates the fronto-parietal network. *Neuroimage, 59,* 1180–1189.
Penhune, V. B., & Steele, C. J. (2012). Parallel contributions of cerebellar, striatal and M1 mechanisms to motor sequence learning. *Behavioural Brain Research, 226,* 579–591.
Perruchet, P., & Pacton, S. (2006). Implicit learning and statistical learning: One phenomenon, two approaches. *Trends in Cognitive Sciences, 10,* 233–238.
Rhodes, B. J., Bullock, D., Verwey, W. B., Averbeck, B. B., & Page, M. P. A. (2004). Learning and production of movement sequences: Behavioral, neurophysiological, and modeling perspectives. *Human Movement Science, 23,* 699–746.
Rogalsky, C., Matchin, W., & Hickok, G. (2008). Broca's area, sentence comprehension, and working memory: An fMRI study. *Frontiers in Human Neuroscience, 2,* 14.
Rosenbaum, D. A., Kenny, S. B., & Derr, M. A. (1983). Hierarchical control of rapid movement sequences. *Journal of Experimental Psychology. Human Perception and Performance, 9,* 86–102.
Rossini, P. M., Barker, A. T., Berardelli, A., Caramia, M. D., Caruso, G., Cracco, R. Q., et al. (1994). Non-invasive electrical and magnetic stimulation of the brain, spinal cord and roots: Basic principles and procedures for routine clinical application. Report of an IFCN committee. *Electroencephalography and Clinical Neurophysiology, 91,* 79–92.
Ruitenberg, M. F. L., Verwey, W. B., Schutter, D. J. L. G., & Abrahamse, E. L. (2014). Cognitive and neural foundations of discrete sequence skill: A TMS study. *Neuropsychologia, 56,* 229–238.
Sakai, K., Hikosaka, O., Miyauchi, S., Takino, R., Sasaki, Y., & Pütz, B. (1998). Transition of brain activation from frontal to parietal areas in visuomotor sequence learning. *Journal of Neuroscience, 18,* 1827–1840.
Sakai, K., Kitaguchi, K., & Hikosaka, O. (2003). Chunking during human visuomotor sequence learning. *Experimental Brain Research, 152,* 229–242.
Santi, A., & Grodzinsky, Y. (2007). Working memory and syntax interact in Broca's area. *Neuroimage, 37,* 8–17.
Schubotz, R. I., & Fiebach, C. J. (2006). Integrative models of Broca's area and the ventral premotor cortex. *Cortex, 42,* 461–463.
Smith, E. E., Jonides, J., & Koeppe, R. A. (1996). Dissociating verbal and spatial working memory using PET. *Cerebral Cortex, 6,* 11–20.
Tanji, J. (2001). Sequential organization of multiple movements: Involvement of cortical motor areas. *Annual Review of Neuroscience, 24,* 631–651.
Tettamanti, M., & Weniger, D. (2006). Broca's area: A supramodal hierarchical processor? *Cortex, 42,* 491–494.
Toni, I., Krams, M., Turner, R., & Passingham, R. E. (1998). The time course of changes during motor sequence learning: A whole-brain fMRI study. *Neuroimage, 61,* 50–61.
Torta, D. M. E., Legrain, V., Algoet, M., Olivier, E., Duque, J., & Mouraux, A. (2013). Theta burst stimulation applied over primary motor and somatosensory cortices produces analgesia unrelated to the changes in nociceptive event-related potentials. *PLoS One, 8,* 1–15.
Tremblay, P. L., Bedard, M. A., Langlois, D., Blanchet, P. J., Lemay, M., & Parent, M. (2010). Movement chunking during sequence learning is a dopamine-dependant process: A study conducted in Parkinson's disease. *Experimental Brain Research, 205,* 375–385.
Ullman, M. T. (2006). Is Broca's area part of a basal ganglia thalamocortical circuit? *Cortex, 42,* 480–485.
Vargha-Khadem, F., Gadian, D. G., Copp, A., & Mishkin, M. (2005). FOXP2 and the neuroanatomy of speech and language. *Nature Reviews Neuroscience, 6,* 131–138.
Verwey, W., & Abrahamse, E. L. (2012). Distinct modes of executing movement sequences: Reacting, associating, and chunking. *Acta Psychologica, 140,* 274–282.
Verwey, W. B. (1996). Buffer loading and chunking in sequential keypressing. *Journal of Experimental Psychology: Human Perception and Performance, 22,* 544–562.
Verwey, W. B. (2001). Concatenating familiar movement sequences: The versatile cognitive processor. *Acta Psychologica, 106,* 69–95.
Verwey, W. B. (2010). Diminished motor skill development in elderly: Indications for limited motor chunk use. *Acta Psychologica, 134,* 206–214.
Verwey, W. B., & Eikelboom, T. (2003). Evidence for lasting sequence segmentation in the discrete sequence-production task. *Journal of Motor Behavior, 35,* 171–181.
Verwey, W. B., Lammens, R., & van Honk, J. (2002). On the role of the SMA in the discrete sequence production task: A TMS study. Transcranial magnetic stimulation. *Neuropsychologia, 40,* 1268–1276.
Watkins, K. E., & Dronkers, N. F. (2002). Behavioural analysis of an inherited speech and language disorder: Comparison with acquired aphasia. *Brain, 125,* 452–464.
Wymbs, N. F., Bassett, D. S., Mucha, P. J., Porter, M. A., & Grafton, S. T. (2012). Differential recruitment of the sensorimotor putamen and frontoparietal cortex during motor chunking in humans. *Neuron, 74,* 936–946.
Zénon, A., & Olivier, E. (2014). Contribution of the basal ganglia to the spoken language: Is speech production like the other motor skills? *Behavioral and Brain Sciences, 37,* 576.
Zénon, A., Sidibé, M., & Olivier, E. (2015). Disrupting the supplementary motor area makes physical effort appear less effortful. *Journal of Neuroscience, 35,* 8737–8744.
Zosso, D., Noirhomme, Q., Davare, M., MacQ, B., Olivier, E., Thiran, J., et al. (2006). Normalization of transcranial magnetic stimulation points by means of atlas registration. *European Signal Processing Conference,* 2–6.